

Extension of SBL Algorithms for the Recovery of Block Sparse Signals with Intra-Block Correlation

Zhilin Zhang, *Student Member, IEEE* and Bhaskar D. Rao, *Fellow, IEEE*

Abstract

We examine the recovery of block sparse signals and extend the framework in two important directions; one by exploiting intra-block correlation and the other by generalizing the block structure. We propose two families of algorithms based on the framework of Block Sparse Bayesian Learning (BSBL). One family, directly derived from the BSBL framework, requires knowledge of the block partition. Another family, derived from an expanded BSBL framework, is based on a weaker assumption about a priori information of the block structure, and can be used in the cases when block partition, block size, block-sparsity are all unknown. Using these algorithms we show that exploiting intra-block correlation is very helpful to improve recovery performance. These algorithms also shed light on how to modify existing algorithms or design new ones to exploit such correlation to improve performance.

Index Terms

Sparse Signal Recovery, Compressed Sensing, Block Sparse Model, Sparse Bayesian Learning (SBL), Intra-Block Correlation

I. INTRODUCTION

Sparse signal recovery and the associated problem of compressed sensing have received much attention in recent years [1]. The model is given by

$$\mathbf{y} = \Phi \mathbf{x} + \mathbf{v}, \quad (1)$$

Z.Zhang and B.D.Rao are with the Department of Electrical and Computer Engineering, University of California, San Diego, La Jolla, CA 92093-0407, USA. Email:{z4zhang,brao}@ucsd.edu. The work was supported by NSF grant CCF-0830612.

where $\mathbf{y} \in \mathbb{R}^{M \times 1}$ is a measurement vector, $\Phi \in \mathbb{R}^{M \times N}$ ($M \ll N$) is a known matrix and any M columns are linearly independent, $\mathbf{x} \in \mathbb{R}^{N \times 1}$ is a sparse signal which we want to recover, and \mathbf{v} is a noise vector. In applications, \mathbf{x} generally have additional structure. A widely studied structure is block/group structure [2]–[4]. With this structure, \mathbf{x} can be viewed as a concatenation of g blocks, i.e.,

$$\mathbf{x} = [\underbrace{x_1, \dots, x_{d_1}}_{\mathbf{x}_1^T}, \dots, \underbrace{x_{d_{g-1}+1}, \dots, x_{d_g}}_{\mathbf{x}_g^T}]^T \quad (2)$$

where $d_i(\forall i)$ are not necessarily identical. Among the g blocks, only k ($k \ll g$) blocks are non-zero but their locations are unknown. It is known that exploiting such block partition can further improve recovery performance.

A number of algorithms have been proposed to recover sparse signals with the block structure. Typical algorithms include Model-CoSaMp [3], Block-OMP [4], and Group-Lasso type algorithms such as the original Group Lasso algorithm [2], Group Basis Pursuit [5], and the Mixed ℓ_2/ℓ_1 Program [6]. These algorithms require knowledge of the block partition (2). Other algorithms such as StructOMP [7], do not need to know the block partition but need to know other a priori information, e.g., the number of non-zero elements in \mathbf{x} . Very recently, CluSS-MCMC [8] and BM-MAP-OMP [9] are proposed, which require very little a priori knowledge.

However, few of existing algorithms consider intra-block correlation, i.e., correlation among amplitudes of elements within each block. In practical applications the intra-block correlation widely exists, such as physiological signals [10] and images. In this work we derive several algorithms that explore and exploit the intra-block correlation to improve performance. These algorithms are based on our recently proposed Block Sparse Bayesian learning (BSBL) framework [11]. Although the framework was initially used to derive algorithms for other related models, it has not been used for the block sparse model (1)-(2). The successes of sparse Bayesian learning methods in past contexts motivates us to consider their extension to this problem and fill this gap.

One contribution of our work is that the proposed algorithms are the first ones in the category that *adaptively* learn and exploit the intra-block correlation. Extensive experiments show that the algorithms developed significantly outperform competitive algorithms. We also propose a promising strategy to incorporate correlation modeling in existing algorithms and improve their performance.

Another contribution is the insight into the effect of the correlation on performance. It is viewed that the multiple measurement vector (MMV) model [12] is a special case of the block sparse model. But we find the effect of intra-block correlation on algorithms based on the block sparse model is quite different from the effect of temporal correlation [11] on algorithms based on the MMV model.

The third contribution is the development of a simple approximate model and corresponding algorithms to solve the problem when the block partition is entirely unknown, which are found empirically to be very effective especially in noisy environments.

In this paper bold symbols are reserved for vectors and matrices. For square matrices $\mathbf{A}_1, \dots, \mathbf{A}_g$, $\text{diag}\{\mathbf{A}_1, \dots, \mathbf{A}_g\}$ denotes a block diagonal matrix with principal diagonal blocks being $\mathbf{A}_1, \dots, \mathbf{A}_g$ in turn. $\text{Tr}(\mathbf{A})$ denotes the trace of \mathbf{A} . $\gamma \succeq \mathbf{0}$ means each element in the vector γ is nonnegative.

Parts of this work has been published in [13].

II. OVERVIEW OF THE BSBL FRAMEWORK

This section briefly describes the Block Sparse Bayesian Learning (BSBL) framework [11], which is the basis of our algorithm development. In this framework, each block $\mathbf{x}_i \in \mathbb{R}^{d_i \times 1}$ is assumed to satisfy a parameterized multivariate Gaussian distribution:

$$p(\mathbf{x}_i; \gamma_i, \mathbf{B}_i) \sim \mathcal{N}(\mathbf{0}, \gamma_i \mathbf{B}_i), \quad i = 1, \dots, g$$

with the unknown hyperparameters γ_i and \mathbf{B}_i . Here γ_i is a nonnegative parameter controlling the block-sparsity of \mathbf{x} . When $\gamma_i = 0$, the i -th block becomes zero. During the learning procedure most γ_i tend to be zero, due to the mechanism of automatic relevance determination [14]. Thus sparsity in the block level is encouraged [11]. $\mathbf{B}_i \in \mathbb{R}^{d_i \times d_i}$ is a positive definite matrix, capturing the correlation structure of the i -th block. Under the assumption that blocks are mutually uncorrelated, the prior of \mathbf{x} is $p(\mathbf{x}) \sim \mathcal{N}(\mathbf{0}, \Sigma_0)$, where Σ_0 is a block-diagonal matrix with the i -th principal block given by $\gamma_i \mathbf{B}_i$. Assume the noise vector satisfies $p(\mathbf{v}) \sim \mathcal{N}(\mathbf{0}, \lambda \mathbf{I})$, where λ is a positive scalar. Therefore the posterior of \mathbf{x} is given by $p(\mathbf{x}|\mathbf{y}; \lambda, \{\gamma_i, \mathbf{B}_i\}_{i=1}^g) = \mathcal{N}(\boldsymbol{\mu}_x, \Sigma_x)$ with $\boldsymbol{\mu}_x = \Sigma_0 \Phi^T (\lambda \mathbf{I} + \Phi \Sigma_0 \Phi^T)^{-1} \mathbf{y}$ and $\Sigma_x = (\Sigma_0^{-1} + \frac{1}{\lambda} \Phi^T \Phi)^{-1}$. Once the hyperparameters $\lambda, \{\gamma_i, \mathbf{B}_i\}_{i=1}^g$ are estimated, the Maximum-A-Posterior (MAP) estimate of \mathbf{x} , denoted by $\hat{\mathbf{x}}$, can be directly obtained from the mean of the posterior, i.e., $\hat{\mathbf{x}} = \boldsymbol{\mu}_x$.

The hyperparameters are generally estimated by a Type II maximum likelihood procedure [14]. This is equivalent to minimizing the following cost function [11] with respect to the hyperparameters

$$\mathcal{L}(\Theta) \triangleq \log |\lambda \mathbf{I} + \Phi \Sigma_0 \Phi^T| + \mathbf{y}^T (\lambda \mathbf{I} + \Phi \Sigma_0 \Phi^T)^{-1} \mathbf{y}, \quad (3)$$

where Θ denotes all the hyperparameters $\lambda, \{\gamma_i, \mathbf{B}_i\}_{i=1}^g$. This framework is called the BSBL framework [11].

Each algorithm derived from this framework includes three learning rules, i.e., the learning rules for γ_i , \mathbf{B}_i , and λ . The learning rule for γ_i is the main body of an algorithm. Different γ_i learning rules lead

to different convergence speed ¹, and determine the possible best recovery performance when optimal values of λ and \mathbf{B}_i are given.

The λ learning rule is important as well. If an optimal (or a good sub-optimal) value for λ cannot be obtained, the recovery performance can be very poor even if the γ_i learning rule could potentially lead to perfect recovery performance.

As for $\mathbf{B}_i(\forall i)$, it can be shown [11] that in noiseless environments, the global minimum of (3) always leads to the true sparse solution no matter what's the value of \mathbf{B}_i . Thus, \mathbf{B}_i only affects local convergence (such as changing the shape of attraction basins of local minima). Therefore, one can impose various constraints on the form of \mathbf{B}_i to achieve better performance and prevent overfitting.

III. ALGORITHMS FOR KNOWN BLOCK PARTITION

In this section we propose three algorithms, which require a priori knowledge of the block partition (2).

A. BSBL-EM: the EM Method

This algorithm can be readily derived from our previous work [11] on the MMV model with suitable adaptation. So we omit the derivation and only present the algorithm. However, several necessary changes, particularly for enhancing the robustness of the learning rules for λ and \mathbf{B}_i have to be made for the block sparsity model considered in this work.

Following the Expectation Maximization (EM) method [11], we can derive the learning rules for γ_i and λ :

$$\gamma_i \leftarrow \frac{1}{d_i} \text{Tr}[\mathbf{B}_i^{-1}(\boldsymbol{\Sigma}_x^i + \boldsymbol{\mu}_x^i(\boldsymbol{\mu}_x^i)^T)], \quad \forall i \quad (4)$$

$$\lambda \leftarrow \frac{\|\mathbf{y} - \boldsymbol{\Phi}\boldsymbol{\mu}_x\|_2^2 + \text{Tr}(\boldsymbol{\Sigma}_x\boldsymbol{\Phi}^T\boldsymbol{\Phi})}{M}, \quad (5)$$

where $\boldsymbol{\mu}_x^i$ is the corresponding i -th block in $\boldsymbol{\mu}_x$ (with the size $d_i \times 1$), and $\boldsymbol{\Sigma}_x^i$ is the corresponding i -th principal diagonal block in $\boldsymbol{\Sigma}_x$ (with the size $d_i \times d_i$). Note that the λ learning rule (5) is not robust in low SNR cases. By numerical study, we empirically find that one of the reasons is the disturbance caused by the off-block-diagonal elements in $\boldsymbol{\Sigma}_x$ and $\boldsymbol{\Phi}^T\boldsymbol{\Phi}$. Therefore, we set their off-block-diagonal elements to zero, leading to the learning rule

$$\lambda \leftarrow \frac{\|\mathbf{y} - \boldsymbol{\Phi}\boldsymbol{\mu}_x\|_2^2 + \sum_{i=1}^g \text{Tr}(\boldsymbol{\Sigma}_x^i(\boldsymbol{\Phi}^i)^T\boldsymbol{\Phi}^i)}{M}, \quad (6)$$

¹The λ learning rule also affects the speed, but its effect is not dominant.

where $\Phi^i \in \mathbb{R}^{M \times d_i}$ is the submatrix of Φ , which correspond to the i -th block of \mathbf{x} . This λ learning rule is better than (5) in generally noisy environments (e.g., SNR < 20dB). In noiseless cases there is no need to use any λ learning rules. Just fixing λ to a small value, e.g., 10^{-10} , can result in satisfactory performance.

Similar to [11], using the EM method we can derive a learning rule for each \mathbf{B}_i . However, we observe that assigning each block with a different \mathbf{B}_i can result in overfitting. When blocks have the same size, an effective strategy to avoid overfitting is parameter averaging [11], i.e., constraining $\mathbf{B}_i = \mathbf{B}, \forall i$. Using this constraint, the learning rule for \mathbf{B} can be derived as follows

$$\mathbf{B} \leftarrow \frac{1}{g} \sum_{i=1}^g \frac{\Sigma_x^i + \mu_x^i (\mu_x^i)^T}{\gamma_i}. \quad (7)$$

However, the algorithm's performance can be improved by further constraining the matrix \mathbf{B} . The idea is to find a positive definite and symmetric matrix $\hat{\mathbf{B}}$ so that it is determined by one parameter but is close to \mathbf{B} especially along the main diagonal and the main sub-diagonal. Further, we find that for many applications modeling elements of a block as a first-order Auto-Regressive (AR) process is sufficient to model the intra-block correlation. In this case, the corresponding covariance matrix of the block is a Toeplitz matrix with the following form:

$$\text{Toeplitz}([1, r, \dots, r^{d-1}]) = \begin{bmatrix} 1 & r & \dots & r^{d-1} \\ \vdots & & & \vdots \\ r^{d-1} & r^{d-2} & \dots & 1 \end{bmatrix} \quad (8)$$

where r is the AR coefficient and d is the block size. Here we constrain $\hat{\mathbf{B}}$ to have this form. Instead of estimating r from the BSBL cost function, we empirically calculate its value by $r \triangleq \frac{m_1}{m_0}$, where m_0 (res. m_1) is the average of the elements along the main diagonal (res. the main sub-diagonal) of the matrix \mathbf{B} in (7).

When blocks have different sizes, the above idea can still be used. First, using the EM method we can derive the rule for each \mathbf{B}_i : $\mathbf{B}_i \leftarrow \frac{1}{\gamma_i} [\Sigma_x^i + \mu_x^i (\mu_x^i)^T]$. Then, for each \mathbf{B}_i we calculate the averages of the elements along the main diagonal and the main sub-diagonal, i.e., m_0^i and m_1^i , respectively, and average m_0^i and m_1^i for all blocks as follows: $\bar{m}_0 \triangleq \sum_{i=1}^g m_0^i$ and $\bar{m}_1 \triangleq \sum_{i=1}^g m_1^i$. Finally, we have $\bar{r} \triangleq \frac{\bar{m}_1}{\bar{m}_0}$, from which we construct $\hat{\mathbf{B}}_i$ for the i -th block:

$$\hat{\mathbf{B}}_i = \text{Toeplitz}([1, \bar{r}, \dots, \bar{r}^{d_i-1}]) \quad (\forall i) \quad (9)$$

We denote the above algorithm by **BSBL-EM**.

B. BSBL-BO: the Bound-Optimization Method

The derived BSBL-EM has satisfactory recovery performance but is very slow. This is mainly due to the EM based γ_i learning rule. For the basic SBL algorithm, Tipping [14] derived a fixed-point based γ_i learning rule to replace the EM based one, which has faster convergence speed but is not robust in some noisy environments. Here we derive a fast γ_i learning rule based on the bound-optimization method (also known as the Majorization-Minimization method) [1], [15]. The algorithm adopting this γ_i learning rule is denoted by **BSBL-BO** (it uses the same learning rules for \mathbf{B}_i and λ as BSBL-EM). It not only has fast convergence speed, but also has satisfactory performance.

Note that the original cost function (3) consists of two terms. The first term $\log |\lambda \mathbf{I} + \Phi \Sigma_0 \Phi^T|$ is concave with respect to $\gamma \succeq \mathbf{0}$, where $\gamma \triangleq [\gamma_1, \dots, \gamma_g]^T$. The second term $\mathbf{y}^T (\lambda \mathbf{I} + \Phi \Sigma_0 \Phi^T)^{-1} \mathbf{y}$ is convex with respect to $\gamma \succeq \mathbf{0}$. Since our goal is to minimize the cost function, we choose to find an upper-bound for the first item and then minimize the upper-bounded cost function.

We use the supporting hyperplane of the first term as its upper-bound. Let γ^* be a given point in the γ -space. We have

$$\begin{aligned} \log |\lambda \mathbf{I} + \Phi \Sigma_0 \Phi^T| &\leq \log |\lambda \mathbf{I} + \Phi \Sigma_0^* \Phi^T| \\ &\quad + \sum_{i=1}^g \text{Tr}((\Sigma_y^*)^{-1} \Phi^i \mathbf{B}_i (\Phi^i)^T) (\gamma_i - \gamma_i^*) \\ &= \sum_{i=1}^g \text{Tr}((\Sigma_y^*)^{-1} \Phi^i \mathbf{B}_i (\Phi^i)^T) \gamma_i + \log |\Sigma_y^*| \\ &\quad - \sum_{i=1}^g \text{Tr}((\Sigma_y^*)^{-1} \Phi^i \mathbf{B}_i (\Phi^i)^T) \gamma_i^* \end{aligned} \quad (10)$$

where $\Sigma_y^* = \lambda \mathbf{I} + \Phi \Sigma_0^* \Phi^T$ and $\Sigma_0^* \triangleq \Sigma_0|_{\gamma=\gamma^*}$. Substituting (10) into the cost function (3) we have

$$\begin{aligned} \mathcal{L}(\gamma) &\leq \sum_{i=1}^g \text{Tr}((\Sigma_y^*)^{-1} \Phi^i \mathbf{B}_i (\Phi^i)^T) \gamma_i \\ &\quad + \mathbf{y}^T (\lambda \mathbf{I} + \Phi \Sigma_0 \Phi^T)^{-1} \mathbf{y} + \log |\Sigma_y^*| \\ &\quad - \sum_{i=1}^g \text{Tr}((\Sigma_y^*)^{-1} \Phi^i \mathbf{B}_i (\Phi^i)^T) \gamma_i^* \\ &\triangleq \tilde{\mathcal{L}}(\gamma) \end{aligned} \quad (11)$$

The function $\tilde{\mathcal{L}}(\gamma)$ is convex over γ , and when $\gamma = \gamma^*$, we have $\mathcal{L}(\gamma^*) = \tilde{\mathcal{L}}(\gamma^*)$. Further, for any γ_{\min} which is the minimum point of $\tilde{\mathcal{L}}(\gamma)$, we have the following relationship: $\mathcal{L}(\gamma_{\min}) \leq \tilde{\mathcal{L}}(\gamma_{\min}) \leq \tilde{\mathcal{L}}(\gamma^*) = \mathcal{L}(\gamma^*)$. This indicates that when we minimize the surrogate function $\tilde{\mathcal{L}}(\gamma)$ over γ , the resulting minimum

point effectively decreases the original cost function $\mathcal{L}(\gamma)$. We can use any convex optimization software to optimize the function (11). However, this takes more time than BSBL-EM and leads to poorer recovery performance in experiments. Therefore, we consider another surrogate function. Using the identity:

$$\mathbf{y}^T(\lambda\mathbf{I} + \Phi\mathbf{\Sigma}_0\Phi^T)^{-1}\mathbf{y} \equiv \min_{\mathbf{x}} \left[\frac{1}{\lambda} \|\mathbf{y} - \Phi\mathbf{x}\|_2^2 + \mathbf{x}^T\mathbf{\Sigma}_0^{-1}\mathbf{x} \right], \quad (12)$$

we have

$$\begin{aligned} \tilde{\mathcal{L}}(\gamma) &= \min_{\mathbf{x}} \frac{1}{\lambda} \|\mathbf{y} - \Phi\mathbf{x}\|_2^2 + \mathbf{x}^T\mathbf{\Sigma}_0^{-1}\mathbf{x} \\ &\quad + \sum_{i=1}^g \text{Tr}((\mathbf{\Sigma}_y^*)^{-1} \Phi^i \mathbf{B}_i (\Phi^i)^T) \gamma_i + \log |\mathbf{\Sigma}_y^*| \\ &\quad - \sum_{i=1}^g \text{Tr}((\mathbf{\Sigma}_y^*)^{-1} \Phi^i \mathbf{B}_i (\Phi^i)^T) \gamma_i^*. \end{aligned}$$

Then, a new function

$$\begin{aligned} \mathcal{G}(\gamma, \mathbf{x}) &\triangleq \frac{1}{\lambda} \|\mathbf{y} - \Phi\mathbf{x}\|_2^2 + \mathbf{x}^T\mathbf{\Sigma}_0^{-1}\mathbf{x} \\ &\quad + \sum_{i=1}^g \text{Tr}((\mathbf{\Sigma}_y^*)^{-1} \Phi^i \mathbf{B}_i (\Phi^i)^T) \gamma_i \\ &\quad + \log |\mathbf{\Sigma}_y^*| - \sum_{i=1}^g \text{Tr}((\mathbf{\Sigma}_y^*)^{-1} \Phi^i \mathbf{B}_i (\Phi^i)^T) \gamma_i^* \end{aligned}$$

is defined, which is the upper-bound of $\tilde{\mathcal{L}}(\gamma)$. Note that $\mathcal{G}(\gamma, \mathbf{x})$ is convex in both γ and \mathbf{x} . It can be easily shown that the solution (γ^\diamond) of $\tilde{\mathcal{L}}(\gamma)$ is the solution $(\gamma^\diamond, \mathbf{x}^\diamond)$ of $\mathcal{G}(\gamma, \mathbf{x})$. Thus, $\mathcal{G}(\gamma, \mathbf{x})$ is our final surrogate cost function.

Taking the derivative of \mathcal{G} with respect to γ_i , we can obtain

$$\gamma_i \leftarrow \sqrt{\frac{\mathbf{x}_i^T \mathbf{B}_i^{-1} \mathbf{x}_i}{\text{Tr}((\Phi^i)^T (\mathbf{\Sigma}_y^*)^{-1} \Phi^i \mathbf{B}_i)}}. \quad (13)$$

Due to this γ_i learning rule, BSBL-BO takes much fewer iterations than BSBL-EM, but has almost the same performance as BSBL-EM.

C. BSBL- ℓ_1 : Hybrid of BSBL and Group-Lasso Type Algorithms

Since the cost function of BSBL-EM and BSBL-BO is a function of γ , they essentially operate in the γ -space. In contrast, most existing algorithms for the block sparse model (1)-(2) directly operate in the \mathbf{x} -space, minimizing a data fit term and a penalty which are both functions of \mathbf{x} . It is interesting to see the relation between our BSBL algorithms and those algorithms.

Using the idea we presented in [16], an extension of the duality space analysis for the basic SBL framework [17], we can transform the BSBL cost function (3) from the γ -space to the \mathbf{x} -space. Since λ and $\mathbf{B}_i(\forall i)$ can be viewed as regularizers, for convenience we first treat them as fixed values.

First, using the identity (12) we can upper-bound the BSBL cost function as follows:

$$\mathfrak{L}(\mathbf{x}, \gamma) = \log |\lambda \mathbf{I} + \Phi \Sigma_0 \Phi^T| + \frac{1}{\lambda} \|\mathbf{y} - \Phi \mathbf{x}\|_2^2 + \mathbf{x}^T \Sigma_0^{-1} \mathbf{x}.$$

By first minimizing over γ and then minimizing over \mathbf{x} , we have:

$$\mathbf{x} = \arg \min_{\mathbf{x}} \left\{ \|\mathbf{y} - \Phi \mathbf{x}\|_2^2 + \lambda g_c(\mathbf{x}) \right\}, \quad (14)$$

with the penalty $g_c(\mathbf{x})$ given by

$$g_c(\mathbf{x}) \triangleq \min_{\gamma \succeq \mathbf{0}} \left\{ \mathbf{x}^T \Sigma_0^{-1} \mathbf{x} + \log |\lambda \mathbf{I} + \Phi \Sigma_0 \Phi^T| \right\}. \quad (15)$$

We now look at the concavity of $g_c(\mathbf{x})$. Since $h(\gamma) \triangleq \log |\lambda \mathbf{I} + \Phi \Sigma_0 \Phi^T|$ is concave and non-decreasing w.r.t. $\gamma \succeq \mathbf{0}$, we have

$$\log |\lambda \mathbf{I} + \Phi \Sigma_0 \Phi^T| = \min_{\mathbf{z} \succeq \mathbf{0}} \mathbf{z}^T \gamma - h^*(\mathbf{z}) \quad (16)$$

where $h^*(\mathbf{z})$ is the concave conjugate of $h(\gamma)$ and can be expressed as $h^*(\mathbf{z}) = \min_{\gamma \succeq \mathbf{0}} \mathbf{z}^T \gamma - \log |\lambda \mathbf{I} + \Phi \Sigma_0 \Phi^T|$. Thus, using (16) we can express (15) as

$$\begin{aligned} g_c(\mathbf{x}) &= \min_{\gamma, \mathbf{z} \succeq \mathbf{0}} \mathbf{x}^T \Sigma_0^{-1} \mathbf{x} + \mathbf{z}^T \gamma - h^*(\mathbf{z}) \\ &= \min_{\gamma, \mathbf{z} \succeq \mathbf{0}} \sum_i \left(\frac{\mathbf{x}_i^T \mathbf{B}_i^{-1} \mathbf{x}_i}{\gamma_i} + z_i \gamma_i \right) - h^*(\mathbf{z}). \end{aligned} \quad (17)$$

Minimizing (17) over γ_i , we have

$$\gamma_i = z_i^{-\frac{1}{2}} \sqrt{\mathbf{x}_i^T \mathbf{B}_i^{-1} \mathbf{x}_i} \quad (\forall i) \quad (18)$$

Plugging it in (17) leads to

$$g_c(\mathbf{x}) = \min_{\mathbf{z} \succeq \mathbf{0}} \sum_i \left(2z_i^{\frac{1}{2}} \sqrt{\mathbf{x}_i^T \mathbf{B}_i^{-1} \mathbf{x}_i} \right) - h^*(\mathbf{z}). \quad (19)$$

Using (19), the problem (14) now becomes:

$$\begin{aligned} \mathbf{x} &= \arg \min_{\mathbf{x}} \|\mathbf{y} - \Phi \mathbf{x}\|_2^2 \\ &\quad + \lambda \left[\min_{\mathbf{z} \succeq \mathbf{0}} \sum_i \left(2z_i^{\frac{1}{2}} \sqrt{\mathbf{x}_i^T \mathbf{B}_i^{-1} \mathbf{x}_i} \right) - h^*(\mathbf{z}) \right]. \end{aligned} \quad (20)$$

To further simplify the expression, we now calculate the optimal values of $z_i^{\frac{1}{2}}$. However, we do not need to calculate the optimal values from the above expression. According to the duality property, from the relation (16) we can directly obtain the optimal value of $z_i^{1/2}$ as follows:

$$\begin{aligned} z_i^{\frac{1}{2}} &= \left(\frac{\partial \log |\lambda \mathbf{I} + \Phi \Sigma_0 \Phi^T|}{\partial \gamma_i} \right)^{\frac{1}{2}} \\ &= \left(\text{Tr} [\mathbf{B}_i \Phi^{iT} (\lambda \mathbf{I} + \Phi \Sigma_0 \Phi^T)^{-1} \Phi^i] \right)^{\frac{1}{2}}. \end{aligned} \quad (21)$$

Note that z_i is a function of γ , while according to (18) γ_i is a function of \mathbf{x}_i (and z_i). This means that the problem (20) should be solved in an iterative way. In the k -th iteration, once having used the updating rules (18) and (21) to obtain $(z_i^{(k)})^{1/2}$, we need to solve the following optimization problem:

$$\mathbf{x}^{(k+1)} = \arg \min_{\mathbf{x}} \|\mathbf{y} - \Phi \mathbf{x}\|_2^2 + \lambda \sum_i w_i^{(k)} \sqrt{\mathbf{x}_i^T \mathbf{B}_i^{-1} \mathbf{x}_i}, \quad (22)$$

where $w_i^{(k)} \triangleq 2(z_i^{(k)})^{1/2}$. And the resulting $\mathbf{x}^{(k+1)}$ will be used to update γ_i and z_i for calculating the solution in the next iteration.

The solution to (22) can be calculated using any group-Lasso type algorithms. To see this, letting $\mathbf{u}_i \triangleq w_i^{(k)} \mathbf{B}_i^{-1/2} \mathbf{x}_i$, $\mathbf{u} \triangleq [\mathbf{u}_1^T, \dots, \mathbf{u}_g^T]^T$, and $\mathbf{H} \triangleq \Phi \cdot \text{diag}\{\mathbf{B}_1^{1/2}/w_1^{(k)}, \dots, \mathbf{B}_g^{1/2}/w_g^{(k)}\}$, the problem (22) can be transformed to the following one

$$\mathbf{u}^{(k+1)} = \arg \min_{\mathbf{u}} \|\mathbf{y} - \mathbf{H} \mathbf{u}\|_2^2 + \lambda \sum_i \|\mathbf{u}_i\|_2.$$

Clearly, each iteration is a standard group-Lasso type problem, while the whole algorithm is an iterative reweighted algorithm.

In the above development we did not consider the learning rules for the regularizers λ and \mathbf{B}_i . In fact, their computation greatly benefits from this iterative reweighted form. Since each iteration is a group-Lasso type problem, the optimal value of λ can be automatically selected in the group Lasso framework [18]. Also, since each iteration provides a block-sparse solution, which is close to the true solution, \mathbf{B}_i can be directly calculated from the solution of the previous iteration. In particular, each non-zero block in the previous solution can be treated as a segment of AR(1) process, and its AR coefficient is thus estimated. The AR coefficients associated with all the non-zero blocks are averaged², and the average value, denoted by \bar{r} , is used to construct each $\hat{\mathbf{B}}_i$ according to (9).

The above algorithm is denoted by **BSBL- ℓ_1** . It can be seen as a hybrid of BSBL algorithms and group-Lasso type algorithms. From one side, it has the ability to adaptively learn and exploit the intra-block correlation for better performance, as BSBL-EM and BSBL-BO. From the other side, since it only

²We find the average step is necessary. Otherwise, the algorithm can have poor performance.

takes few iterations (generally about 2 to 5 iterations in noisy environments) and each iteration can be implemented by any efficient group-Lasso type algorithm, it is much faster and is especially suitable for large-scale datasets, compared to BSBL-EM and BSBL-BO.

The algorithm also provides insights if we want to equip group-Lasso type algorithms with the ability to exploit intra-block correlation for better recovery performance. We can consider this iterative reweighted method and change the ℓ_2 norm of \mathbf{x}_i , i.e., $\|\mathbf{x}_i\|_2$, to the Mahalanobis-distance type measure $\sqrt{\mathbf{x}_i^T \mathbf{B}_i^{-1} \mathbf{x}_i}$.

IV. ALGORITHMS FOR UNKNOWN BLOCK PARTITION

Now we extend the previous framework to derive algorithms when block partition is unknown. For the algorithm development, *we assume that all the blocks are of equal size h and the non-zeros blocks are arbitrarily located*. Later we will see that the approximation of equal block size is not limiting. Note that though the resulting algorithms are not very sensitive to the choice of h , algorithmic performance can be further improved if a suitable value of h is selected. We will comment more on h later.

Given the identical block size h , there are $p \triangleq N - h + 1$ possible blocks in \mathbf{x} , which overlap each other. The i -th block starts at the i -th element of \mathbf{x} and ends at the $(i + h - 1)$ -th element. All the non-zero elements of \mathbf{x} lie in some of these blocks. Similar to Section III, for the i -th block, we assume it satisfies a multivariate Gaussian distribution with the mean given by $\mathbf{0}$ and the covariance matrix given by $\gamma_i \mathbf{B}_i$, where $\mathbf{B}_i \in \mathbb{R}^{h \times h}$. So the prior of \mathbf{x} has the form: $p(\mathbf{x}) \sim \mathcal{N}_x(\mathbf{0}, \Sigma_0)$. Note that due to the overlapping locations of these blocks, Σ_0 is no longer a block diagonal matrix. It has the structure that each $\gamma_i \mathbf{B}_i$ lies along the principal diagonal of Σ_0 and overlaps other $\gamma_j \mathbf{B}_j$ in neighbor. Thus, we cannot directly use the previous BSBL framework and need to make some modifications.

To facilitate the use of the BSBL framework, we expand the covariance matrix Σ_0 as follows:

$$\tilde{\Sigma}_0 = \text{diag}\{\gamma_1 \mathbf{B}_1, \dots, \gamma_p \mathbf{B}_p\} \in \mathbb{R}^{ph \times ph} \quad (23)$$

Note that now $\gamma_i \mathbf{B}_i$ does not overlap other $\gamma_j \mathbf{B}_j$ ($i \neq j$). The $\tilde{\Sigma}_0$ implies the decomposition of \mathbf{x}

$$\mathbf{x} = \sum_{i=1}^p \mathbf{E}_i \mathbf{z}_i, \quad (24)$$

where $E\{\mathbf{z}_i\} = \mathbf{0}$, $E\{\mathbf{z}_i \mathbf{z}_j^T\} = \delta_{i,j} \gamma_i \mathbf{B}_i$ ($\delta_{i,j} = 1$ if $i = j$; otherwise, $\delta_{i,j} = 0$), and $\mathbf{z} \triangleq [\mathbf{z}_1^T, \dots, \mathbf{z}_p^T]^T \sim \mathcal{N}_z(\mathbf{0}, \tilde{\Sigma}_0)$. $\mathbf{E}_i \in \mathbb{R}^{N \times h}$ is a zero matrix except that the part from its i -th row to $(i + h - 1)$ -th row is replaced by the identity matrix \mathbf{I} . Then the original model (1) can be expressed as:

$$\mathbf{y} = \sum_{i=1}^p \Phi \mathbf{E}_i \mathbf{z}_i + \mathbf{v} \triangleq \mathbf{A} \mathbf{z} + \mathbf{v}, \quad (25)$$

where $\mathbf{A} \triangleq [\mathbf{A}_1, \dots, \mathbf{A}_p]$ with $\mathbf{A}_i \triangleq \Phi \mathbf{E}_i$. Now the new model (25) is a block sparse model and can be solved by the BSBL framework. Thus, following the development of BSBL-EM, BSBL-BO, and BSBL- ℓ_1 , we obtain algorithms for this expanded model, which are called **EBSBL-EM**, **EBSBL-BO**, and **EBSBL- ℓ_1** , respectively.

In the above development we assumed that all the blocks have the same size h , which is known. However, this assumption is not crucial for practical use. When the size of a non-zero block of \mathbf{x} , say \mathbf{x}_j , is larger or equal to h , it can be recovered by a set of (overlapped) \mathbf{z}_i ($i \in \mathcal{S}$, \mathcal{S} is a non-empty set). When the size of \mathbf{x}_j is smaller than h , it can be recovered by a \mathbf{z}_i for some i . In this case, since \mathbf{z}_i is larger, the elements in \mathbf{z}_i with global locations (i.e., the indexes in \mathbf{x}) different from those of elements in \mathbf{x}_j are very close to zero. In Section V, we will see different values of h lead to similar performance. The insight also implies that we can partition a signal into blocks of equal (or almost equal) size h and then perform BSBL algorithms in this situation. But generally EBSBL algorithms are less sensitive to h than BSBL algorithms.

Note that our approach using the expanded model in the situation when block partition is unknown is quite different from existing approaches [7]–[9]. An advantage of our approach is that it simplifies the algorithm, which, in turn, increases robustness in noisy environments, as shown in Section V. Another benefit of this approach is that it facilitates the exploitation of intra-block correlation. Since the intra-block correlation widely exists in practical signals and exploiting such correlation can significantly improve performance, our approach is more competitive than existing approaches.

V. EXPERIMENTS

Due to space limit, we only present some representative experimental results based on computer simulations (Experiments on real-world data can be found in [10]). Every set of experiment settings consisted of 400 trials. The matrix Φ in all the experiments was generated as a zero mean random Gaussian matrix with columns normalized to unit ℓ_2 norm. In noisy experiments the Normalized Mean Square Error (NMSE) was used as a performance index, defined by $\|\hat{\mathbf{x}} - \mathbf{x}_{\text{gen}}\|_2^2 / \|\mathbf{x}_{\text{gen}}\|_2^2$, where $\hat{\mathbf{x}}$ was the estimate of the true signal \mathbf{x}_{gen} ; in noiseless experiments the *success rate* was used as a performance index, defined as the percentage of successful trials in the 400 trials (A successful trial was defined as the one when $\text{NMSE} \leq 10^{-5}$).

In noiseless experiments, BSBL- ℓ_1 chose the Mixed ℓ_2/ℓ_1 Program to perform its every iteration; in noisy experiments, it chose the Group Basis Pursuit. For all of our algorithms, when calculating r , the formula $r \triangleq \text{sign}(\frac{m_1}{m_0}) \min\{|\frac{m_1}{m_0}|, 0.99\}$, instead of the original formula $r = \frac{m_1}{m_0}$, was used to ensure the

calculated r is feasible (not larger than 1 or smaller than -1). The same modification goes to \bar{r} .

The Matlab codes and demo files of BSBL algorithms and EBSBL algorithms can be downloaded at <https://sites.google.com/site/researchbyzhang/bsbl>.

A. Phase Transition

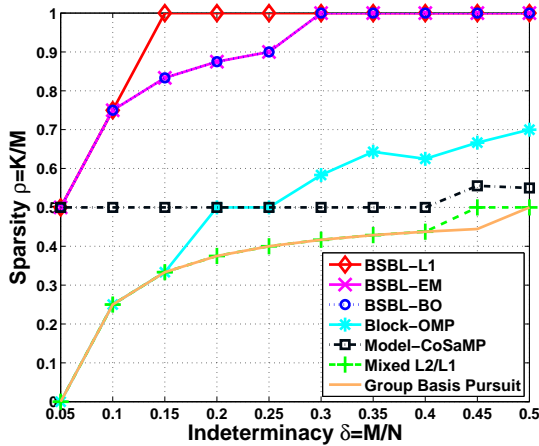
We first examined the empirical phase transitions [19] for our three BSBL algorithms, Block-OMP, Model-CoSaMP, the Mixed ℓ_2/ℓ_1 Program, and Group Basis Pursuit when exactly recovering a block sparse signal in noiseless environments. The phase transition is generally used to illustrate how sparsity level (defined as $\rho = K/M$, where K is the number of non-zero elements) and indeterminacy (defined as $\delta = M/N$) affect algorithms' success in exact recovery of sparse signals. Each point on the plotted phase transition curve corresponds to the success rate of an algorithm larger than or equal to 0.99 in 400 trials; above the curve the algorithm's success rate sharply drops, while below the curve the success rate is 1.

In the experiment the indeterminacy $\delta = M/N$ ran from 0.05 to 0.5 with N fixed to 1000. For each M and N , a block sparse signal was generated, which consisted of 40 blocks with identical block size 25. The number of non-zero blocks varied from 1 to 20, and thus the number of non-zero elements varied from 25 to 500. Locations of the non-zero blocks were determined randomly. The block partition was known to the algorithms, but the number of non-zero blocks and their locations were unknown to the algorithms. Each non-zero block was generated by a multivariate Gaussian distribution with zero mean and covariance matrix Σ_{gen} . By changing the covariance matrix, thus changing intra-block correlation, we could study the effect of intra-block correlation on phase transitions of the algorithms.

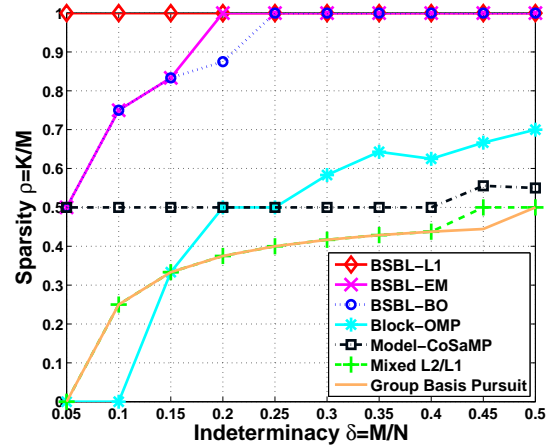
We first considered the situation when there was no correlation within each non-zero block (i.e., $\Sigma_{\text{gen}} = \mathbf{I}$). The empirical phase transition curves of all the algorithms are shown in Fig.1 (a). Clearly, our three BSBL algorithms have the best performance. It is worth noting that when $\delta \geq 0.15$, BSBL- ℓ_1 exactly recovers block sparse signals with $\rho = 1$ with a high success rate (≥ 0.99).

The results become more interesting when intra-block correlation was 0.95 (i.e., $\Sigma_{\text{gen}} = \text{Toeplitz}([1, 0.95, \dots, 0.95^{24}])$). The empirical phase transition curves are shown in Fig.1 (b), where all the three BSBL algorithms have improved performance. BSBL- ℓ_1 can exactly recover sparse signals with $\rho = 1$ even $\delta < 0.15$. And BSBL-EM and BSBL-BO now can exactly recover sparse signals with $\rho = 1$ when $\delta \geq 0.25$. Opposite to BSBL algorithms, the compared four algorithms show little change in performance when the intra-block correlation changes from 0 to 0.95.

These results are very interesting and surprising, since this may be the first time that an algorithm



(a) Intra-Block Correlation: 0



(b) Intra-Block Correlation: 0.95

Fig. 1. Empirical 99% phase transitions of all the algorithms (a) when there was no correlation within each non-zero block, and (b) when the intra-block correlation was 0.95. Each point on a phase transition curve corresponds to the success rate larger than or equal to 0.99.

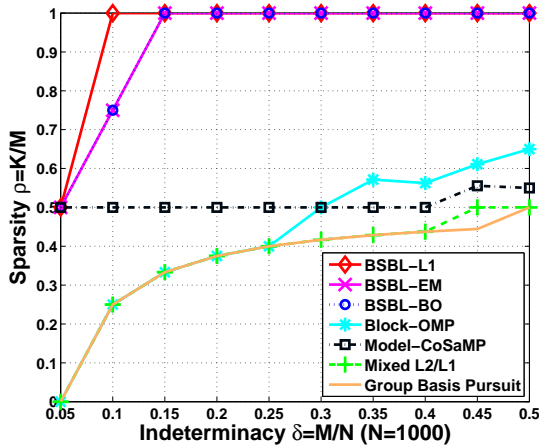
shows the ability to recover a block sparse signal of M non-zero elements from M measurements with a high success rate (≥ 0.99). Obviously, exploiting block structure and intra-block correlation plays a crucial role here. Further, these results indicate the advantages of the BSBL framework.

Figure 2 (a) and (b) shows the empirical phase transitions of all the algorithms when elements of each non-zero block satisfy Bimodal Rayleigh distribution (i.e., $|\mathbf{x}_i|$ satisfies a Rayleigh distribution with the parameter $\sigma = 3$) and Laplacian distribution (with zero mean and the scale parameter $b = 10$), respectively. We can see that the superiority of the BSBL algorithms is obvious over a wide range of distributions.

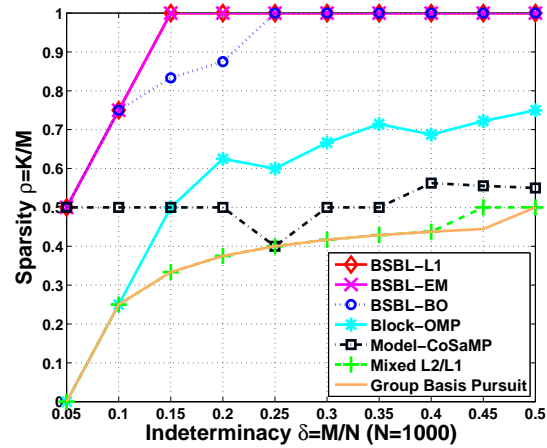
B. Benefit from Exploiting Intra-Block Correlation

The above results have hinted the benefit from exploiting intra-block correlation. To see this clearer, another noiseless experiment was carried out. The matrix Φ was of the size 100×300 . The signal consisted of 75 blocks with identical size. Only 20 of the blocks were non-zero. All the non-zero blocks had the same intra-block correlation (generated as in Section V-A) with the value ranging from -0.99 to 0.99. Different from the above experiment, each non-zero block was further normalized to unit ℓ_2 norm in order to remove the interference caused by different ℓ_2 norms of the blocks.

BSBL-EM, BSBL-BO and BSBL- ℓ_1 were performed in two ways. First, they adaptively learned and



(a) Bimodal Rayleigh



(b) Laplacian

Fig. 2. Empirical 99% phase transitions of all the algorithms when elements in each non-zero block satisfied (a) a Bimodal Rayleigh distribution, and (b) a Laplacian distribution. Each point on a phase transition curve corresponds to the success rate larger than or equal to 0.99.

exploited the intra-block correlation. In the second case, they ignored the correlation, i.e., setting $\mathbf{B}_i = \mathbf{I}(\forall i)$.

The results are shown in Fig.3 (a). First, we see that exploiting intra-block correlation greatly improves the performance of the BSBL algorithms. Second, when not exploiting intra-block correlation, the performance of the BSBL algorithms shows no obvious relation to the correlation. Note that the second observation is different from the observation on *temporal correlation* in the MMV model, where we find that if temporal correlation is *not exploited*, algorithms have poorer performance with increasing temporal correlation values [11]. The second phenomenon can also be seen from the performance of existing algorithms in Section V-A, where their performance has little change when intra-block correlation dramatically varies.

In the above experiment all the non-zero blocks had the same intra-block correlation. A natural question is, “when the intra-block correlation of each non-zero block largely differs, can our proposed algorithms be still effective?” To answer it, we considered three correlation cases. In the first case the intra-block correlation of each non-zero block was uniformly chosen from -1 to 1; in the second case, uniformly chosen from 0 to 1; and in the third case, uniformly chosen from 0.7 to 1. BSBL-EM was performed in two ways, i.e., exploiting the correlation and ignoring the correlation. The results in the three cases are shown in Fig.3 (b), indicated by ‘Case 1’, ‘Case 2’, and ‘Case 3’, respectively. We can see in Case

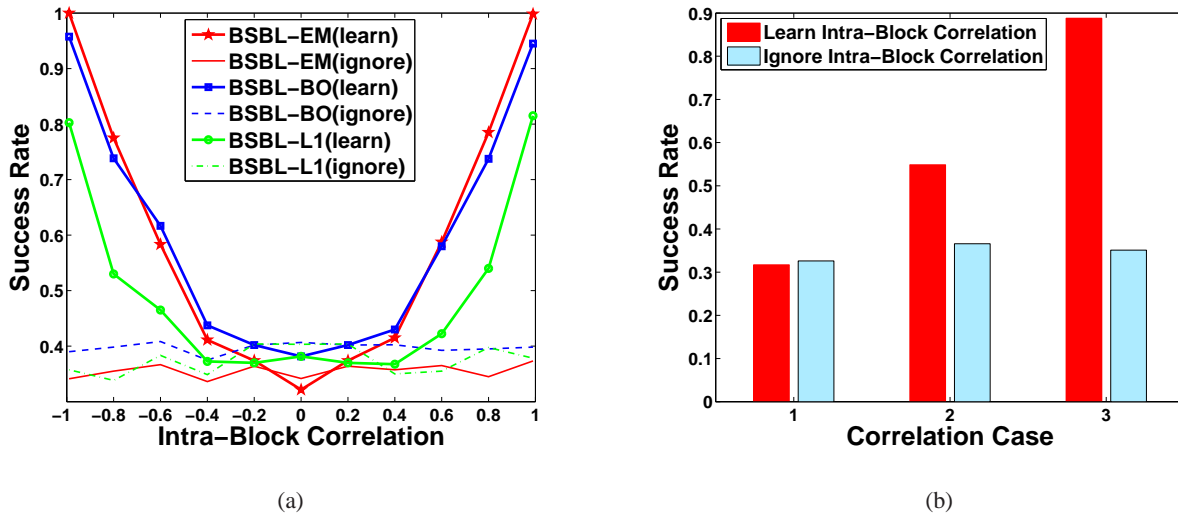


Fig. 3. (a) shows the benefit from exploiting intra-block correlation. (b) shows the performance of BSBL-EM in three correlation cases.

3 the benefit from exploiting the correlation is significant, while in Case 1 the benefit disappears (but exploiting correlation is not harmful). However, note that Case 1 rarely happens in practice. In fact, in many practical problems the intra-block correlation of all non-zero blocks tends to be positive and high, which corresponds to Case 2 and Case 3.

Experimental results on real-world data which show the benefit from exploiting intra-block correlation are presented in [10].

C. Performance in Noisy Environments

We compared the three BSBL algorithms, Mixed ℓ_2/ℓ_1 Program, Group Lasso, and Group Basis Pursuit at different noise levels. In this experiment $M = 128$ and $N = 512$. The generated block sparse signal was partitioned into 64 blocks with identical block size 8. Seven blocks were non-zero, generated as in Section V-A. The intra-block correlation of each block varied from 0.8 to 1 randomly. Gaussian white noise was added so that the SNR, defined by $\text{SNR}(\text{dB}) \triangleq 20 \log_{10}(\|\Phi \mathbf{x}_{\text{gen}}\|_2 / \|\mathbf{v}\|_2)$, stepped from 5 dB to 25 dB for each generated signal. As a benchmark result, the ‘oracle’ result was calculated, which was the least-square estimate of \mathbf{x}_{gen} given its true support.

The results are shown in Fig.4 (a), where our algorithms have much better performance, especially the performance curves of BSBL-EM and BSBL-BO almost overlap the ‘Oracle’ performance curve. The phenomenon that BSBL- ℓ_1 has slightly poorer performance at low SNR and high SNR situations is due

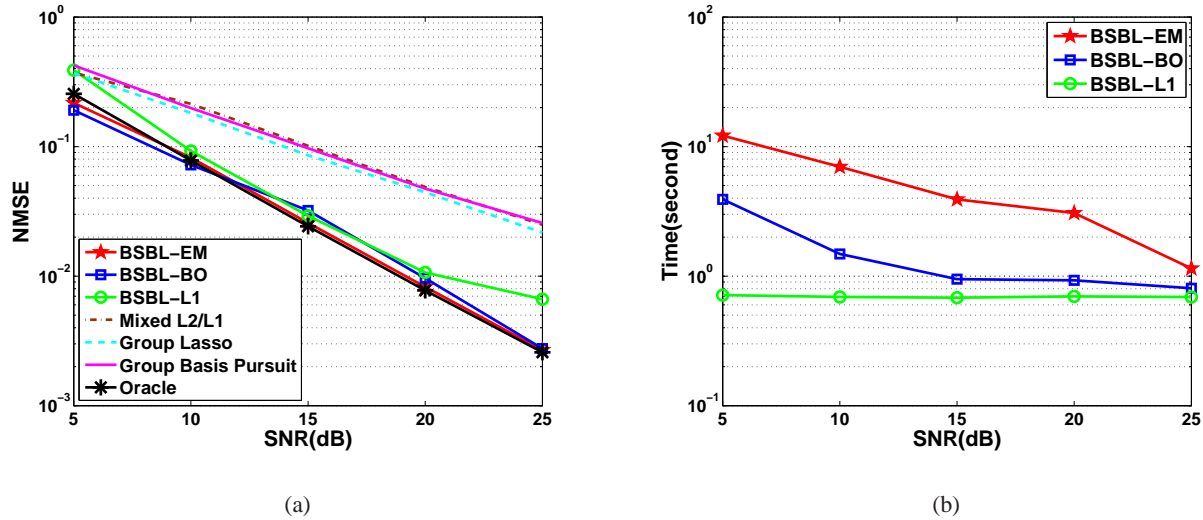


Fig. 4. (a) Performance comparison in different noise levels. (b) Speed comparison of the three BSBL algorithms in the noisy experiment.

to some sub-optimal default parameters in the Group Basis Pursuit program. We find the phenomenon disappears when using other software. Figure 4 (b) gives the speed comparison of the three algorithms in a laptop with 2.8G CUP and 6G RAM. Clearly, BSBL- ℓ_1 was the fastest among the three, due to the use of Group Basis Pursuit in its every iteration.

D. Performance When Block Partition Is Unknown

We set up a noisy experiment when block partition was unknown and compared all of our algorithms with StructOMP (given the number of non-zero elements), BM-MAP-OMP (given the true noise variance), and CluSS-MCMC. The matrix Φ was of the size 192×512 . The signal \mathbf{x}_{gen} had g_0 non-zero blocks with random size and random locations (not overlapping). g_0 was varied from 2 to 10. The total number of non-zero elements in \mathbf{x}_{gen} was fixed to 48. The intra-block correlation in each block randomly varied from 0.8 to 1. SNR was 15 dB. As we stated in Section IV, h is not crucial for practical use. To see this, we set $h = 4$ and $h = 8$ for our algorithms. But to prevent from being over-crowded when plotting performance curves, we only display BSBL-EM and EBSBL-BO with $h = 4$ and $h = 8$. We also performed T-MSBL [11] here. Note that when T-MSBL is used in the block sparse model, it can be viewed as a special case of BSBL-EM with each block size being 1. The results are shown in Fig.5. Clearly, our algorithms outperformed StructOMP, CluSS-MCMC, and BM-MAP-OMP. And for both BSBL-EM and EBSBL-BO, setting $h = 4$ or $h = 8$ led to similar performance.

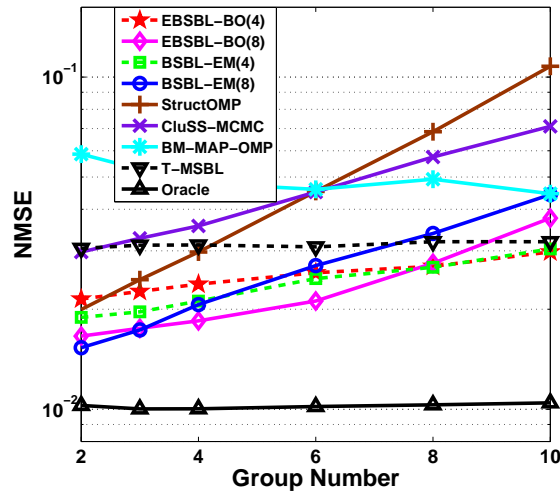


Fig. 5. Performance comparison when block partition was unknown.

VI. CONCLUSION

Based on the block sparse Bayesian learning framework and its extension, we proposed a number of algorithms to recover block sparse signals both when the block partition is known and is unknown. Motivated by the fact that intra-block correlation widely exists in practical block sparse signals, these proposed algorithms have the ability to explore and exploit the intra-block correlation for better performance. Experiments show that these algorithms significantly outperform existing algorithms. The derived algorithms also suggest that the iterative reweighted framework is a promising method for Group-Lasso type algorithms to exploit the intra-block correlation.

REFERENCES

- [1] M. Elad, *Sparse and redundant representations*. Springer Verlag, 2010.
- [2] M. Yuan and Y. Lin, "Model selection and estimation in regression with grouped variables," *J. R. Statist. Soc. B*, vol. 68, pp. 49–67, 2006.
- [3] R. G. Baraniuk, V. Cevher, M. F. Duarte, and C. Hegde, "Model-based compressive sensing," *IEEE Trans. on Information Theory*, vol. 56, no. 4, pp. 1982–2001, 2010.
- [4] Y. C. Eldar, P. Kuppinger, and H. Bolcskei, "Block-sparse signals: uncertainty relations and efficient recovery," *IEEE Trans. on Signal Processing*, vol. 58, no. 6, pp. 3042–3054, 2010.
- [5] E. Van Den Berg and M. Friedlander, "Probing the pareto frontier for basis pursuit solutions," *SIAM Journal on Scientific Computing*, vol. 31, no. 2, pp. 890–912, 2008.
- [6] Y. C. Eldar and M. Mishali, "Robust recovery of signals from a structured union of subspaces," *IEEE Trans. on Information Theory*, vol. 55, no. 11, pp. 5302–5316, 2009.

- [7] J. Huang, T. Zhang, and D. Metaxas, "Learning with structured sparsity," in *ICML*, 2009, pp. 417–424.
- [8] L. Yu, H. Sun, J. P. Barbot, and G. Zheng, "Bayesian compressive sensing for cluster structured sparse signals," *Signal Processing*, vol. 92, no. 1, pp. 259–269, 2012.
- [9] T. Peleg, Y. Eldar, and M. Elad, "Exploiting statistical dependencies in sparse representations for signal recovery," *IEEE Trans. on Signal Processing*, vol. 60, no. 5, pp. 2286–2303, 2012.
- [10] Z. Zhang, T.-P. Jung, S. Makeig, and B. D. Rao, "Low energy wireless body-area networks for fetal ECG telemonitoring via the framework of block sparse Bayesian learning," *IEEE Trans. on Biomedical Engineering (submitted)*, 2012. [Online]. Available: arXiv:1205.1287v2[stat.ML]
- [11] Z. Zhang and B. D. Rao, "Sparse signal recovery with temporally correlated source vectors using sparse bayesian learning," *IEEE Journal of Selected Topics in Signal Processing*, vol. 5, no. 5, pp. 912–926, 2011.
- [12] S. F. Cotter, B. D. Rao, K. Engan, and K. Kreutz-Delgado, "Sparse solutions to linear inverse problems with multiple measurement vectors," *IEEE Trans. on Signal Processing*, vol. 53, no. 7, pp. 2477–2488, 2005.
- [13] Z. Zhang and B. D. Rao, "Recovery of block sparse signals using the framework of block sparse Bayesian learning," in *Proc. of the 37th International Conference on Acoustics, Speech, and Signal Processing (ICASSP 2012)*, Japan, 2012, pp. 3345–3348.
- [14] M. E. Tipping, "Sparse Bayesian learning and the relevance vector machine," *J. of Mach. Learn. Res.*, vol. 1, 2001.
- [15] P. Stoica and P. Babu, "SPICE and LIKES: Two hyperparameter-free methods for sparse-parameter estimation," *Signal Processing*, 2012.
- [16] Z. Zhang and B. D. Rao, "Exploiting correlation in sparse signal recovery problems: Multiple measurement vectors, block sparsity, and time-varying sparsity," in *ICML 2011 Workshop on Structured Sparsity: Learning and Inference*, 2011.
- [17] D. Wipf and S. Nagarajan, "Iterative reweighted ℓ_1 and ℓ_2 methods for finding sparse solutions," *IEEE Journal of Selected Topics in Signal Processing*, vol. 4, no. 2, pp. 317–329, 2010.
- [18] R. Tibshirani, J. Bien, J. Friedman, and et al, "Strong rules for discarding predictors in lasso-type problems," *J. R. Statist. Soc. B*, vol. 74, 2012.
- [19] D. Donoho and J. Tanner, "Observed universality of phase transitions in high-dimensional geometry, with implications for modern data analysis and signal processing," *Philosophical Transactions of the Royal Society A*, vol. 367, no. 1906, pp. 4273–4293, 2009.